Involvement of ASIP/PAR-3 in the promotion of epithelial tight junction formation

Tomonori Hirose[1], Yasushi Izumi[1], Yoji Nagashima[2], Yoko Tamai-Nagai[1], Hidetake Kurihara[3], Tatsuo Sakai[3], Yukari Suzuki[1], Tomoyuki Yamanaka[1], Atsushi Suzuki[1], Keiko Mizuno[1] and Shigeo Ohno[1,*]

[1]Department of Molecular Biology and [2]Department of Pathology, Yokohama City University School of Medicine, Kanazawa-ku, Yokohama 236-0004, Japan
[3]Department of Anatomy, Juntendo University School of Medicine, Bunkyo-ku, Tokyo 113-8421, Japan
*Author for correspondence (e-mail: ohnos@med.yokohama-cu.ac.jp)

Accepted 10 April 2002
Journal of Cell Science 115, 2485-2495 (2002) © The Company of Biologists Ltd

Summary

The mammalian protein ASIP/PAR-3 interacts with atypical protein kinase C isotypes (aPKC) and shows overall sequence similarity to the invertebrate proteins *C. elegans* PAR-3 and *Drosophila* Bazooka, which are crucial for the establishment of polarity in various cells. The physical interaction between ASIP/PAR-3 and aPKC is also conserved in *C. elegans* PAR-3 and PKC-3 and in *Drosophila* Bazooka and DaPKC. In mammals, ASIP/PAR-3 colocalizes with aPKC and concentrates at the tight junctions of epithelial cells, but the biological meaning of ASIP/PAR-3 in tight junctions remains to be clarified. In the present study, we show that ASIP/PAR-3 staining distributes to the subapical domain of epithelial cell-cell junctions, including epithelial cells with less-developed tight junctions, in clear contrast with ZO-1, another tight-junction-associated protein, the staining of which is stronger in cells with well-developed tight junctions. Consistently, immunogold electron microscopy revealed that ASIP/PAR-3 concentrates at the apical edge of tight junctions, whereas ZO-1 distributes alongside tight junctions. To clarify the meaning of this characteristic localization of ASIP, we analyzed the effects of overexpressed ASIP/PAR-3 on tight junction formation in cultured epithelial MDCK cells. The induced overexpression of ASIP/PAR-3, but not its deletion mutant lacking the aPKC-binding sequence, promotes cell-cell contact-induced tight junction formation in MDCK cells when evaluated on the basis of transepithelial electrical resistance and occludin insolubilization. The significance of the aPKC-binding sequence in tight junction formation is also supported by the finding that the conserved PKC-phosphorylation site within this sequence, ASIP-Ser827, is phosphorylated at the most apical tip of cell-cell contacts during the initial phase of tight junction formation in MDCK cells. Together, our present data suggest that ASIP/PAR-3 regulates epithelial tight junction formation positively through interaction with aPKC.

Key words: ASIP/PAR-3, Atypical PKC, Epithelial tight junction, Epithelial cell polarity

Introduction

Epithelial cells play essential roles in separating biological compartments to regulate homeostasis and maintain physiological functions in separate biological environments. These functions are established by organized junctional complexes, cytoskeletal architecture, distinct plasma membrane domains, and highly polarized protein sorting (Yeaman et al., 1999; Balda and Matter, 1998). One form of junctional complex, tight junctions (TJs), is characterized by conventional electron microscopy as a series of fusion points on the cell membranes of adjacent cells, and in freeze-fracture electron microscopy appears as intramembranous anastomosing strands, TJ strands (Farquhar and Palade, 1963; Staehelin, 1973). TJs function as an intercellular barrier to regulate paracellular permeability in vertebrate epithelial and endothelial cells. In addition, TJs comprise one of the essential structures for the establishment of epithelial cell polarity, because TJ strands provide physical fences within the membrane bilayer that prevent the intermixing of membrane domains, and thus maintain cell surface asymmetry (Mitic and Anderson, 1998; Tsukita et al., 1999). Furthermore, several lines of evidence suggest that TJ serve as specific sites for vesicle targeting to establish and maintain the epithelial polarity of the cell membrane (Yeaman et al., 1999).

We have previously identified a novel protein with three PDZ domains, atypical PKC isotype-specific interacting protein (ASIP), which colocalizes with aPKC at the cell-cell junctions of confluent fibroblastic and epithelial cells. Immunogold electron microscopy revealed that ASIP localizes at the TJ of rat intestinal epithelium (Izumi et al., 1998). In addition, ASIP/PAR-3 shows significant overall sequence similarity to two invertebrate polarity proteins, *C. elegans* PAR-3 and *Drosophila* Bazooka, and one of the highly conserved regions in ASIP/PAR-3 is critical for the interaction with the kinase domain of aPKC (Izumi et al., 1998; Etemad-Moghadam et al., 1995; Kuchinke et al., 1998). Furthermore, the physical interaction between ASIP/PAR-3 and aPKC is conserved in *C. elegans* PAR-3 and PKC-3, as well as in *Drosophila* Bazooka and DaPKC (Izumi et al., 1998; Tabuse et al., 1998; Wodarz et al., 2000). Immunofluorescent and genetic analyses of *C. elegans* and *Drosophila* revealed that each pair of proteins, PAR-3 and PKC-3 or Bazooka and

DaPKC, shows asymmetric colocalization in various cells undergoing asymmetric cell division, and that the two are mutually dependent on each other for correct localization to regulate spindle orientation and the distribution of other cell fate determinants (Tabuse et al., 1998; Wodarz et al., 2000). These data suggest that an evolutionarily conserved protein complex is involved in the regulation of various cell polarity and differentiation events; however, the physiological meaning of the aPKC–ASIP/PAR-3 interaction in mammals remains to be clarified.

In the present study, we show that ASIP/PAR-3 distributes to apical cell-cell junctions of various rat epithelial cells, but in a manner clearly different from ZO-1, another TJ-associated protein. While ZO-1 staining patterns show a good correlation with the development level of TJ, ASIP/PAR-3 can be detected in all epithelial cell-cell junctions examined, including those without highly developed TJ strands. Together with the fact that aPKC is critical for the establishment of TJs in epithelial cells (Suzuki et al., 2001), these data led us to analyze the possibility that ASIP/PAR-3 might play a regulatory role in TJ formation and/or maintenance, rather than serving only as a structural element. Indeed, our functional and biochemical analyses revealed that the overexpression of ASIP/PAR-3, but not its deletion mutant lacking the aPKC-binding sequence, promotes TJ formation in epithelial MDCK cells. Furthermore, the aPKC-binding sequence includes two highly conserved PKC phosphorylation consensus sites [Ser827 and Ser829 (Izumi et al., 1998)], suggesting that this function of ASIP/PAR-3 is mediated through phosphorylation by aPKC. This possibility is further supported by data showing that ASIP/PAR-3 is phosphorylated at Ser827 and concentrates to the apical-most cell-cell contacts of MDCK cells during TJ formation. Together, these results provide the first evidence supporting the involvement of ASIP/PAR-3 in the promotion of epithelial TJ formation through interaction with aPKC.

Materials and Methods

Materials

The MDCK Tet-Off cell line [established from the MDCK type II cell line (Barth et al., 1997)], pTRE (GenBank accession no. U89931) and pTK-Hyg (GenBank accession no. U40398), carrying the hygromycin-resistance gene, were purchased from Clontech (Palo Alto, CA). Tetracycline (TC) and doxycycline (DC) were purchased from Sigma (St Louis, MO).

pTREHis/L-ASIP WT encodes a splice variant (K.M. and S.O., unpublished) of the rat ASIP sequence lacking amino acid (a.a.) residues 740-742 and 857-871 fused downstream of the six histidine residues and an 11-a.a. sequence from the T7 gene 10-leader sequence. pTERHis/L-ASIP ΔPB encodes a T7-tagged chimera of a splice variant of mouse (N-terminal 989 a.a.) and rat ASIP/PAR-3 (C-terminal 315 a.a.) lacking residues 740-742 and the aPKC-binding sequence [residues 827-856 (K.M. and S.O., unpublished)]. The expression of both of these proteins is under the control of the tetracycline repressible transactivator (Gossen and Bujard, 1992).

Rabbit anti-ASIP/PAR-3 antibodies were raised against a GST fusion protein of the aPKC-binding region (C2-3; residues 712-936), the third PDZ domain (P2-2; residues 584-708), and the C-terminal region (A2-2; residues 1124-1337) as described (Izumi et al., 1998). Antibodies against the specific C-terminal tail of the splice variant of ASIP/PAR-3 and ASIP/PAR-3 phosphorylated at Ser827 (anti-S827-P) were raised against synthetic peptides corresponding to residues 1023-1034 (NH_2-MFSLAKLKPEKR-COOH) and residues 822-832 phosphorylated at Ser827 (NH_2-CGFGRQpSMSEKR-COOH), respectively. Each rabbit antibody produced against a KLH-coupled antigen was affinity purified (Y.T.-N. and S.O., unpublished). The mouse anti-ZO-1 monoclonal antibody was kindly provided by S. Tsukita (Kyoto University, Kyoto, Japan) or purchased from Zymed Laboratories (South San Francisco, CA). Rabbit anti-occludin polyclonal antibody, rabbit anti-T7 polyclonal antibody (Omni probe), mouse anti-T7 monoclonal antibody, FITC-conjugated secondary antibodies and Cy3-conjugated secondary antibodies were purchased from Zymed Laboratories, Santa Cruz Biotechnology (Santa Cruz, CA), Novagen (Madison, WI), E. Y. Laboratories (San Mateo, CA) and Amersham Life Science (Arlington Heights, IL), respectively.

Gel electrophoresis and western blot analysis

Samples of various rat organs and intestinal epithelial cell scrapings (Saxon et al., 1994) were subjected to SDS-PAGE (Laemmli, 1970) and electrotransferred to a polyvinylidene difluoride membrane, which was then soaked in 5% nonfat milk and 10% calf serum in PBS (137 mM NaCl, 8.1 mM Na_2HPO_4, 2.68 mM KCl and 1.47 mM KH_2PO_4). The membrane was incubated first with affinity purified anti-ASIP antibody (C2-3AP, A2-2AP or Yap) and then with horseradish peroxidase-conjugated secondary antibody. Antibodies were detected by a chemiluminescence ECL plus system (Amersham Life Science).

Immunofluorescence microscopy

Adult rat forestomach (Izumi et al., 1998) and duodenum (Saxon et al., 1994) were prepared as described. A kidney from a 12-week-old rat was rinsed in ice-cold PBS, cut into small blocks and immersed in paraformaldeyde-lysine-periodate fixative (McLean and Nakane, 1974) for 30 minutes at 4°C. After fixation, the tissue was washed three times with PBS containing 50 mM NH_4Cl for 15 minutes at 4°C, and cryoprotected in 30% (w/v) sucrose in PBS for 18 hours at 4°C. The tissue blocks were embedded and frozen in Tissue Tek OCT compound. The frozen specimens were cut in a cryostat to a thickness of about 4 μm, mounted on glass slides, and air-dried. The sections were permeabilized in PBS containing 0.2% Triton X-100 for 5 minutes at room temperature, and then the nonspecific sites were blocked with PBS containing 10% calf serum for 30 minutes at room temperature. The sections were incubated for 45 minutes at 37°C with primary antibodies diluted in TBST (20 mM Tris-HCl, pH 8.0, 150 mM NaCl, 0.05% Tween-20) containing 0.1% bovine serum albumin, and washed three times for 5 minutes with TBST. After the first incubation, the sections were incubated for 45 minutes at 37°C with secondary antibodies (FITC-conjugated goat anti-rabbit and Cy3-conjugated anti-mouse antibodies) and washed three times for 5 minutes with TBST.

MDCK cells grown on 1.0 cm^2 Transwell-Clear™ filters (#3460, Corning Coster, Cambridge, MA) were fixed in 2% formaldehyde in PBS for 10 minutes at room temperature, washed twice in PBS, permeabilized in PBS containing 0.5% Triton X-100 and 100 mM glycine for 5 minutes at room temperature, and subjected to immunofluorescence detection as described above.

The samples were mounted in PBS containing 50% VECTASHIELD mounting medium (Vector Labs, Burlingame, CA) and examined under a fluorescence microscope (BX40, Olympus) equipped with a CCD camera (Princeton Instruments, Trenton, NJ) or a confocal microscope system (Nikon E-600 microscope equipped with BioRad μ-Radiance). Images were arranged and labeled using Adobe PhotoShop (Adobe Systems, San Jose, CA).

Immunoelectron microscopy

Rat kidneys were perfused with 1% paraformaldehyde fixative buffered with 0.1 M sodium phosphate buffer (PB, pH 7.4) and

immersed in the same fixative for 30 minutes at 4°C. The samples were rinsed with 5% sucrose for 30 minutes at 4°C. Tissue samples were then infiltrated with 40% polyvinylpyrrolidone (Sigma)/2.3 M sucrose buffered with 0.1 M PB, embedded on nails, and frozen quickly in liquid nitrogen. Ultrathin cryosections were cut with a Leica Ultracut UCT equipped with a Leica EM FCS cryoattachment (Wien, Austria) at –110°C. Sections were transferred to Formvar-coated nickel grids (150 mesh). Subsequent incubation steps were carried out by floating the grids on droplets of the filtered solution. Free aldehyde groups were quenched with PBS-0.01 M glycine, and the sections were incubated overnight with PBS containing 10% fetal bovine serum (FBS) and affinity purified rabbit anti-ASIP antibody (C2-3AP, 1:50 dilution). Next, the grids were incubated with anti-rabbit IgG coupled to 5 nm gold (diluted 1:100, British BioCell, Cardiff, UK) for 1 hour. Double immunogold staining with ASIP and ZO-1 antibody was also carried out. In brief, ultrathin cryosections of aldehyde-fixed kidney were cut as described above. The sections were incubated with affinity-purified rabbit anti-ASIP antibody (C2-3AP, 1:50 dilution with PBS containing 10% FBS) and mouse monoclonal anti-ZO-1 antibody (Zymed Laboratories, 1:100 dilution) and then incubated with 10 nm gold-conjugated goat anti-rabbit IgG (diluted 1:100, British BioCell) and 5 nm gold-conjugated goat anti-mouse IgG (diluted 1:100, British BioCell). After immunostaining, the samples were fixed in 2.5% glutaraldehyde buffered with 0.1 M PB (pH 7.4). The sections were then contrasted with 2% uranyl acetate solution for 20 minutes, and absorption-stained with 3% polyvinyl alcohol containing 0.2% uranyl acetate for 20 minutes. All sections were observed with a JEOL 1230-EX electron microscope.

Cell cultures

Parental MDCK Tet-Off cells [(Barth et al., 1997) #C3017-1, Clontech, Palo Alto, CA) and established stable clones were grown in Dulbecco's modified Eagle's medium (DMEM; GibcoBRL, Rockville, MD) containing 10% FBS, penicillin, and streptomycin at 37°C in an air/5% CO_2 atmosphere at constant humidity. The MDCK cell lines were cultured with or without 10 ng/ml of DC for at least 3 days before experiments.

Selection of MDCK cell lines stably expressing mutant ASIPs

The parental MDCK Tet-Off cells were co-transfected with expression plasmids for ASIP/PAR-3 (pTREHis/L-ASIP WT or pTERHis/L-ASIP ΔPB) and pTK-Hyg. The overall procedures followed mainly the previously described method (Jou and Nelson, 1998). 9 μg ASIP/PAR-3 plasmid, 3 μg pTK-Hyg, and 40 μl lipofectamine PLUS reagent (GibcoBRL, Rockville, MD) were mixed in 1160 μl of serum-free DMEM containing 50 μM Ca^{2+} (SF-LCM) at room temperature for 30 minutes; 1.2 ml of SF-LCM containing 5% lipofectamine reagent (GibcoBRL) was then added and the mixture was incubated for an additional 15 minutes. The mixture was diluted with 9.6 ml of SF-LCM and added to the 1.5×10^6 cells plated in each of two 10 cm dishes; the cells were in log phase growth and had been maintained in 2 μg/ml of TC. After 6 hours at 37°C, the medium was replaced with DMEM containing 10% FBS and 2 μg/ml of TC, and the cells were incubated for a further 24 hours and passaged to fifteen 10 cm dishes in medium containing 200 μg/ml hygromycin B (Wako, Osaka, Japan). After selection for 10 days, the surviving colonies were isolated using cloning rings, and exogenous ASIP/PAR-3 expression was assessed in each colony by western blotting 48 hours after the removal of TC. Positive clones were expanded in the presence of TC, divided into aliquots and stored in liquid nitrogen.

Measurement of transepithelial electric resistance (TER) and cell growth

Cells were trypsinized, suspended in DMEM containing 10% FBS with or without 10 ng/ml of DC, and plated on 1.0 cm^2 Transwell-Clear™ (#3460) filters at the indicated cell densities and on P-60 dishes. TER was measured using a Millicell-ERS (Millipore Corp.), and cell growth was assessed by counting the number of cells on the P-60 dishes at different times after plating. TER values were calculated by subtracting the values of blank Transwell-Clear™ filters, and normalized to the area of the monolayers. Every point is the mean ±s.e.m of three groups of cells on independent filters.

Calcium switch and occludin fractionation

MDCK stable clones were plated on 3.9 cm^2 Transwell-Clear™ (#3450) filters at a density of 2×10^5 cells/cm^2, incubated for 20 hours in normal calcium medium, rinsed once with PBS, and changed from medium to low calcium medium [LCM; DMEM supplemented with 5 μM $CaCl_2$ and 5% FBS that had been dialyzed against PBS (Gumbiner and Simons, 1986)]. After a 20 hour incubation in LCM, the level of $CaCl_2$ was adjusted back to 1.8 mM for calcium switch. Cells were harvested with PBS at different times after switching, and the cell pellets were frozen at –80°C. NP-40-insoluble fractions were prepared by following the method described previously (Sakakibara et al., 1997). Briefly, the cells were lysed in 700 μl of ice-cold NP-40-IP buffer (25 mM Hepes/NaOH, pH 7.4, 150 mM NaCl, 1% NP-40, 50 mM NaF, 1 mM Na_3VO_4, 4 mM EDTA, 1 mM PMSF, 10 μg/ml leupeptin, 2 μg/ml aprotinin, 0.5 mM benzamidine) by 30-minute rotation at 4°C. After centrifugation (10,000 ***g*** for 30 minutes) the pellet was redissolved in 87.5 μl of 2× SDS-sample buffer (Laemmli, 1970), and then subjected to western blotting analyses with anti-ASIP antibody (C2-3AP) and anti-occludin pAb (Zymed). The levels of NP-40-insoluble occludin were detected by chemiluminescence ECL (Amersham Life Science), quantified directly with an LAS-1000 plus system (FUJI Photo Film, Tokyo, Japan), and then normalized to the amount of tubulin in each lane.

Results

ASIP/PAR-3 is expressed in various tissues and distributes to the subapical domains of epithelial cell-cell junctions in a manner different from that of ZO-1

Our previous study revealed that there are at least two ASIP/PAR-3 isoforms with molecular masses of 180 kDa and 150 kDa, which are identifiable with two independent antibodies against the aPKC-binding domain (C1-3/C2-3) or the third PDZ domain (P2-2) by western blotting analysis of cultured mammalian cells. Both isoforms are detected in MDCKII and COS cells, whereas only the 180 kDa isoform is observed in NIH3T3 cells (Izumi et al., 1998). Subsequent studies revealed that the 180 kDa ASIP/PAR-3 corresponds to the full length product while the 150 kDa ASIP/PAR-3 is a major splicing variants with a shorter C-terminal tail (Fig. 1A) (Lin et al., 2000). As a first step to obtain information about the physiological function of ASIP/PAR-3 in mammalian tissues, we tried to extend our knowledge of the expression and cellular localization of ASIP/PAR-3 in a variety of rat tissues. We established three independent affinity-purified antibodies against the aPKC-binding region (C2-3AP), the C-terminal region of full-length ASIP/PAR-3 (A2-2AP), and the specific C-terminal sequence in the shorter splice variants (Yap; Fig. 1A). As shown in Fig. 1B, western blotting analysis with C2-3AP revealed 180 kDa bands detected predominantly in lung, glandular stomach, prostate, ovary and uterus that show the same migration rate as the full-length ASIP/PAR-3 transcript (ASIP180k) expressed exogenously in COS1 cells. In addition, smaller bands around 150 kDa are detected in intestinal epithelial cells, kidney and

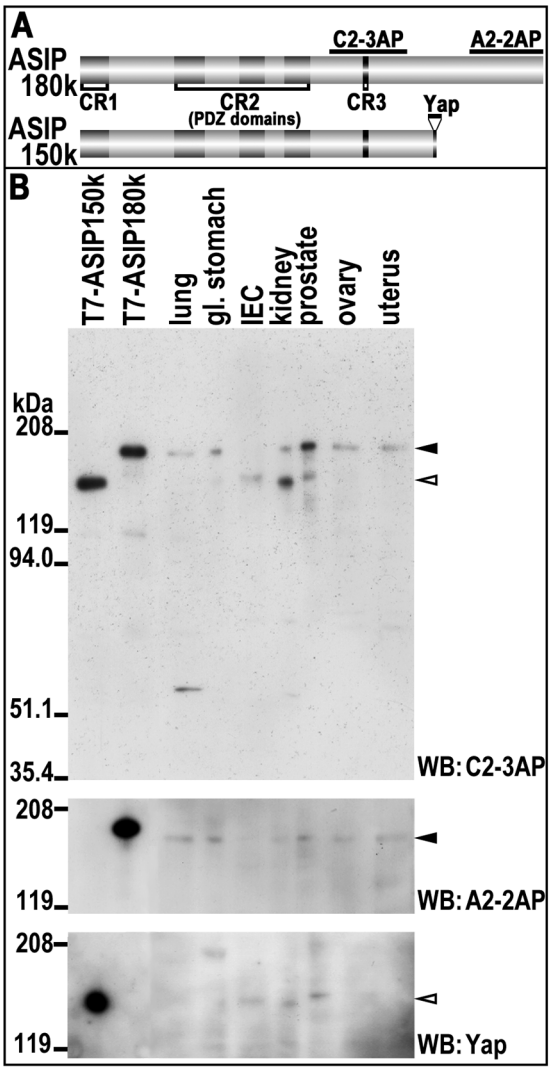

Fig. 1. (A) Full length ASIP/PAR-3 (ASIP180k) and its splice variant with a shorter C-termini (ASIP150k). The region recognized by each antibody (C2-3AP, A2-2AP and Yap) is indicated; Yap recognizes the specific C-terminal sequence of ASIP150k. CR, conserved region. (B) Expression of ASIP/PAR-3 in various rat tissues. Total extracts from various rat tissues (lung, glandular stomach, kidney, prostate, ovary, uterus), intestinal epithelial cell scrapings (IEC), and COS1 cells transfected with T7-ASIP150k or T7-ASIP180k as positive controls were subjected to SDS-PAGE (8% polyacrylamide gel) followed by western blot analysis with the affinity-purified anti-ASIP antibodies (C2-3AP, A2-2AP and Yap). C2-3AP recognizes bands of 180 kDa (filled arrowheads; lung, glandular stomach, kidney, prostate, ovary and uterus) and 150/160 kDa (unfilled arrowheads; IEC, kidney and prostate), which are recognized by A2-2AP and Yap, respectively.

prostate. Importantly, bands of 180 kDa and about 150 kDa are recognized by A2-2AP and Yap, respectively. These data indicate that the 180 kDa and 150/160 kDa bands correspond to the full length product of ASIP/PAR-3 and its splice variants with shorter C-termini, respectively. Since ASIP/PAR-3 has been shown to have several minor, small deleted regions that presumably originate from alternative splicing (Joberty et al., 2000; K.M. and S.O., unpublished), the slight difference in the molecular masses of the ASIP/PAR-3 bands may reflect tissue-dependent differential expression of these variants. Taken together, these results suggest that ASIP/PAR-3 is expressed ubiquitously but with tissue-dependent sequence modifications that preserve the aPKC-binding region.

We next examined the distribution of ASIP/PAR-3 in a variety of rat epithelial tissues in comparison with another TJ-associated protein, ZO-1 (Stevenson et al., 1986). The specificity of ASIP/PAR-3 staining was confirmed by the abolishment of the signal by the corresponding antigen, or by the identity of the staining pattern with another affinity-purified antibody against the third PDZ domain of ASIP/PAR-3 (P2-2AP), or both (data not shown). One of the most striking differences between the distribution of ASIP/PAR-3 and ZO-1 is the lack of ASIP/PAR-3 staining in the cell-cell contact region of endothelial cells in every epithelial tissue examined (forestomach, small intestine, renal cortex) where ZO-1 is highly expressed (Fig. 2B,F, arrowheads) (Stevenson et al., 1986).

In epithelial cells, the ASIP/PAR-3 staining pattern is similar to that of ZO-1. In general, ASIP/PAR-3 (Fig. 2, green) distributes to the subapical domain of every epithelial cell-cell junction examined. Furthermore, from the basal to the granular layers of the stratified squamous epithelium in forestomach, where characteristic TJ are not established, the stainings of both ASIP/PAR-3 and ZO-1 are mostly detected as non-continuous patterns in the cell-cell contact regions and appear as punctate patterns in the cytoplasm (Fig. 2A-C). These results are reminiscent of previous observations in MDCKII cells where ASIP/PAR-3 and ZO-1 show cytoplasmic punctate distributions during the reconstitution of TJ (Izumi et al., 1998; Rajasekaran et al., 1996). However, a close comparison of the staining patterns reveals an intriguing difference between the distribution of ASIP/PAR-3 and ZO-1 in epithelial cells. Although ASIP/PAR-3 signals can be detected throughout the epithelial layer, their levels are slightly lower in the basal layer and the most superficial zone of the granular layer. In contrast, ZO-1 signal level is very low in the basal layer and increase from the spinous to the granular layer (Fig. 2C), as reported previously (Morita et al., 1998). Considering the correlation between the levels of epithelial cell differentiation and the depth of the epithelial layer (Fig. 2D), these results suggest that ASIP/PAR-3 staining level is relatively higher in cells undergoing differentiation, whereas ZO-1 staining increases with epithelial cell differentiation in the forestomach. In agreement with this observation, a merged view of ASIP/PAR-3–ZO-1 staining in the small intestine demonstrates yellow signals in the crypts (Fig. 2G, unfilled arrowheads) and orange signals in the villus (asterisk), indicating that the signal intensity of ASIP/PAR-3 (green) in immature epithelial cells is relatively higher than that of ZO-1 (red). Thus, ASIP/PAR-3 exists in cell-cell junctions at relatively higher levels than ZO-1 in differentiating epithelial cells with less developed TJ strands in the forestomach and small intestine (Marcial et al., 1984).

A difference between ASIP/PAR-3 and ZO-1 is also observed in epithelial cells in renal tubules (Fig. 2I-K). There is no significant difference between the signal intensities of ASIP/PAR-3 in the proximal and distal renal tubules (Fig. 2I). In contrast, the signal intensity of ZO-1 is much higher in distal rather than proximal renal tubules (Fig. 2J), consistent with a previous report that ZO-1 signals correlate with the number of TJ strands (Fig. 2L) (Schnabel et al., 1990).

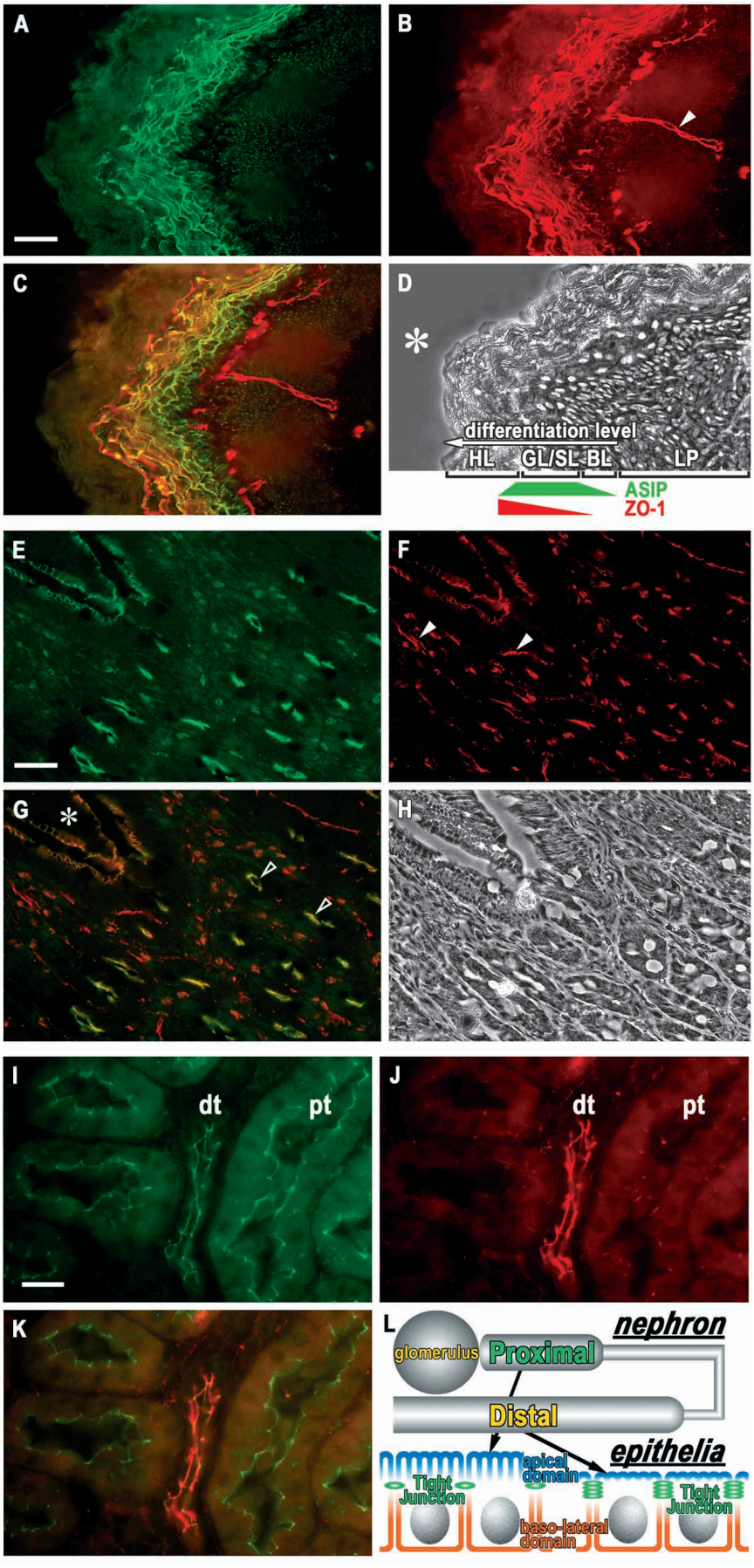

Fig. 2. ASIP/PAR-3 distributes at the cell-cell junctions of various rat epithelial cells in a manner different from that of ZO-1. The differential distributions of ASIP/PAR-3 and ZO-1 are compared in rat forestomach (A-C), small intestine (E-G), and renal cortex (I-K). The samples were double stained with affinity-purified anti-ASIP antibody (C2-3AP, green) and anti-ZO-1 (red). In merged views (C,G,K), the yellow and orange signals show the co-localizations of ASIP/PAR-3 and ZO-1. In stratified squamous epithelium, ASIP/PAR-3 localizes at cell-cell junctions from the basal layer to the granular layer, and some cytoplasmic punctate patterns are observed (A). The localization of ZO-1 in the same field as in A is shown in B. The signal intensity of ZO-1 in the cell-cell junctions was much higher in the spinous layer than in the basal layer. ZO-1 is also detected in blood vessels (B, arrowhead), whereas ASIP/PAR-3 is not. As shown in the merged view (C) and indicated schematically in D, the relative signal intensities of ASIP/PAR-3 and ZO-1 differ along with epithelial differentiation. (D) Phase contrast image. Asterisk, lumen; BL, basal layer; GL, granular layer; HL, horny layer; LP, lamina propria; SL, spinous layer. In small intestine, ASIP/PAR-3 is concentrated in the subapical domain of epithelial cell-cell junctions (E) in a manner different from that of ZO-1 (F). As indicated in (B), ZO-1 signals are also detected in blood vessels (F, arrowheads). Unfilled arrowheads in G indicate that the signal intensity of ASIP/PAR-3 (green) in crypts is relatively higher than that of ZO-1 (red), whereas ZO-1 signal intensities are relatively higher in villus (asterisk). (H) Phase contrast image of the same field as E. As shown in I-K, the signal intensity of ASIP/PAR-3 (green) in proximal renal tubules (pt) is the same as in distal tubules (dt); however, that of ZO-1 (red) is much higher in distal renal tubules (dt) than proximal tubules (pt). (L) Schematic structure of proximal and distal renal tubules in a nephron. The number of TJ strands in epithelial cells of the distal renal tubule is much higher than in the proximal tubule. Bars, 40 μm (A), 20 μm (E), 10 μm (I).

In order to clarify this characteristic distribution of ASIP/PAR-3 at the ultrastructural level, the localization of ASIP/PAR-3 and ZO-1 was investigated in renal tubule epithelial cells by immunogold electron microscopy (Fig. 3). In both epithelial cells with deep TJ in the distal tubules (Fig. 3A) and those with relatively shallow TJ in the proximal tubules (Fig. 3B), ASIP/PAR-3 localizes at the cytoplasmic surfaces of TJ. Intriguingly, not all of the TJ are decorated with gold particles for ASIP/PAR-3: ASIP/PAR-3 is always detected at the upper edges of TJ (Fig. 3A-D) and is frequently observed at the lower edges of TJ (Fig. 3A,B). By double-label

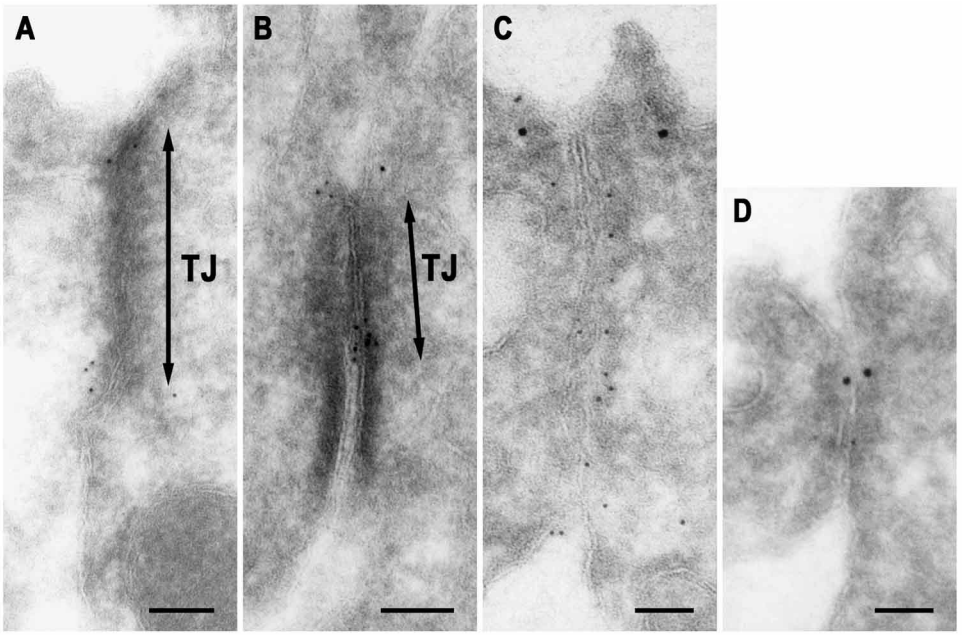

Fig. 3. Immunogold electron microscopy of ASIP/PAR-3 (A-D) and ZO-1 (C,D) in epithelial cells of distal (A,C) and proximal (B,D) renal tubules. Ultrathin cryosections of rat renal tubular epithelial cells were labeled with anti-ASIP/PAR-3 pAb (A,B; 5 nm gold particles). In both the distal (A) and proximal (B) tubules, gold particles for ASIP/PAR-3 are concentrated exclusively in the cytoplasm of TJ. Gold particles are constantly observed at the apical edge of TJ, and are also frequently found at the basal edge of TJ. (C,D) Double immunolabeling of renal tubular epithelium for ASIP/PAR-3 and ZO-1. In contrast to ASIP/PAR-3 (10 nm gold particles), ZO-1 (5 nm gold particles) distributes alongside TJ in the distal (C) and proximal (D) tubules. Apical is up and basal is down in these figures (A-D). TJ, tight junction. Bars, 100 nm.

immunogold electron microscopy, this characteristic localization of ASIP/PAR-3 contrasts sharply with that of ZO-1, which distributes alongside TJs as reported previously (Kurihara et al., 1992) (Fig. 3C and data not shown). Therefore, the amount and distribution of ASIP/PAR-3 do not necessarily correlate with the level of TJ development in the epithelial cells examined here, whereas those of ZO-1 depend closely on the number of TJ strands, the structural basis of TJ. Together with the fact that the kinase activity of aPKC, the binding partner of ASIP/PAR-3, is indispensable for the development of TJs in epithelial cells (Suzuki et al., 2001), our observations led us to investigate the possibility that ASIP/PAR-3 might play a regulatory role in establishing and/or maintaining TJ structure, rather than serving only as a structural component of TJ.

Induced overexpression of ASIP/PAR-3 in MDCK cells promotes the development of transepithelial electrical resistance (TER) after plating

To examine the possibility that ASIP/PAR-3 regulates epithelial TJ formation, we evaluated the effect of the overexpression of ASIP/PAR-3 or its mutant on the formation and function of TJ. For this purpose, we employed stable transformants in which ASIP/PAR-3 could be induced by tetracycline or doxycycline deprivation (Gossen and Bujard, 1992; Barth et al., 1997). We prepared two different T7-tagged expression plasmids for L-ASIPs; L-ASIP WT has the aPKC-binding sequence, whereas L-ASIP ΔPB does not (Fig. 4A). The regulation of the expression of each protein in the established cell line was evaluated by western blotting and immunofluorescence with the antibody against the T7-tag, and we found that the expression of L-ASIP WT or ΔPB was

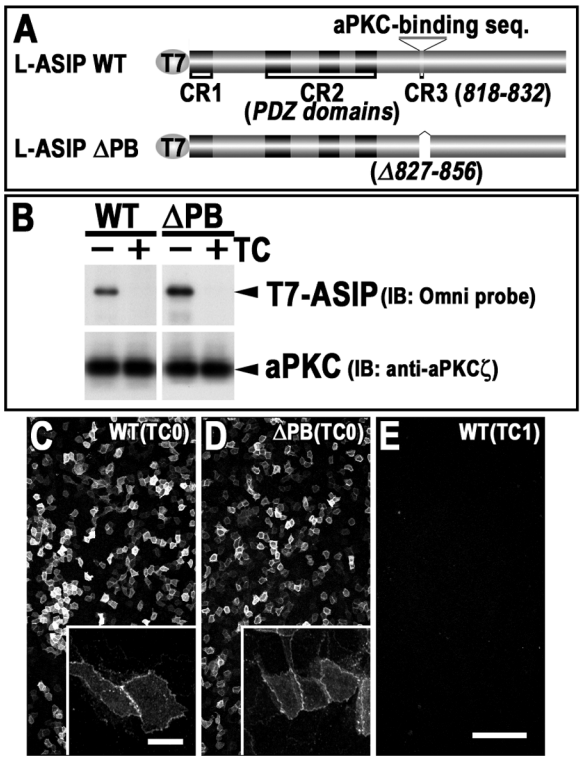

Fig. 4. Characterization of MDCK Tet-Off cell lines expressing T7-tagged L-ASIP WT or ΔPB. (A) Schematic structures of the constructs. The aPKC-binding sequence is found in L-ASIP WT but not in L-ASIP ΔPB. (B) Each cell line was cultured with (+) or without (–) 1.0 μg/ml of tetracycline (TC), and 5×10^4 cells/lane were subjected to western blot analysis with the T7-tag-specific antibody (Omni probe) or anti-aPKCζ antibody. The expression of T7-tagged ASIP/PAR-3 in each cell line was strongly induced by the withdrawal of TC, whereas 1.0 μg/ml of TC completely repressed the expression to under the detectable levels. (C-E) Immunofluorescent images show that the overexpressed T7-tagged ASIPs localize mainly at cell-cell contacts of MDCK cells cultured without TC (TC0). Confluent monolayers of MDCK cells expressing T7-L-ASIP WT (C) or T7-L-ASIP ΔPB (D) were labeled by the Omni probe pAb. 1 μg/ml of TC (TC1) completely repressed the expressions of L-ASIP WT (E) and L-ASIP ΔPB (not shown). Bars, 100 μm; 10 μm (inset).

completely repressed to under the detectable level by 1.0 μg/ml of tetracycline (TC) (Fig. 4B,E) or 10 ng/ml of doxycycline (DC) (Fig. 5G). We also assessed the distribution of each T7-tagged ASIP/PAR-3 and the homogeneity of its expression level by immunofluorescence. In MDCK cell lines overexpressing L-ASIP WT or ΔPB, even though the type of exogenously expressed ASIP/PAR-3 is different, both T7-tagged ASIPs preferentially concentrate at cell-cell contacts as endogenous ASIP/PAR-3, and there is no significant difference in homogeneity of protein expression between the two MDCK cell lines overexpressing L-ASIP (Fig. 4C,D).

We analyzed the development of transepithelial electrical resistance (TER) using these cell lines. Since TER essentially reflects paracellular resistance regulated by TJ, de novo formation of TJ can be followed through the development of TER after plating (Cereijido et al., 1998). The TER of MDCK cell monolayers initially increases with time after plating and begins to decrease after the cells become confluent (Jou et al., 1998). First, since cell proliferation is a key factor affecting TER development, we examined whether the overexpression of ASIP/PAR-3 can alter cell proliferation; however, we found no significant difference between cells cultured in the presence or absence of the repressor (10 ng/ml of DC) in any cell line examined (Fig. 5A-C). By contrast, the induced overexpression of L-ASIP WT reproducibly results in the promotion of the early phase of TER development after cell plating at subconfluent density (1.5×10^5 cells/cm^2; Fig. 5D, asterisks). Although the two types of ASIP/PAR-3 are expressed in virtually the same way and remain constant during cell proliferation (Fig. 5G), the overexpression of L-ASIP ΔPB has no effect on TER development (Fig. 5E). In addition, we confirmed that the depletion of DC itself does not promote but

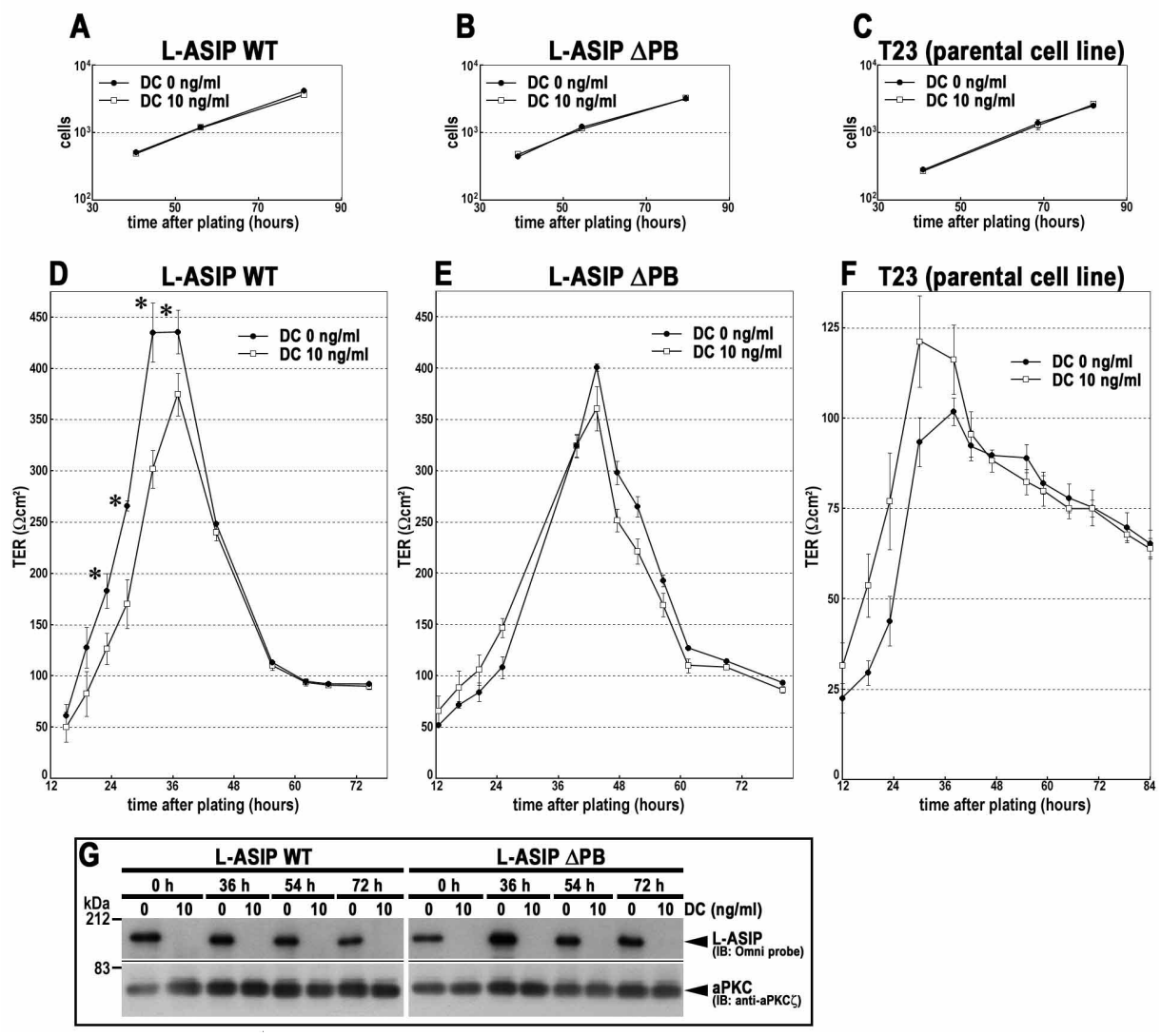

Fig. 5. Induced overexpression of ASIP/PAR-3 accelerates TER development after cell plating. (A-C) There is no significant difference in cell growth between cells cultured with or without 10 ng/ml of doxycycline (DC). (D-F) TER development of each cell line was measured at different times after plating on Transwell-Clear^{TM} filters at a density of 1.5×10^5 cells/cm^2. Cells were maintained with or without 10 ng/ml of DC for at least 3 days before plating. Every point is the mean±s.e.m. of three groups of cells on independent filters. *P*-values were calculated with a two-sided *t*-test and statistical significance was considered at $P<0.05$ (D, asterisks). (G) Expressions of the T7-tagged ASIPs and endogenous aPKC at the different times after plating. Cells were maintained with or without 10 ng/ml of DC and 5×10^4 cells/lane were subjected to western blot analysis with the T7-tag-specific antibody (Omni probe) and anti-aPKCζ antibody.

rather suppresses TER development in the parental cell line (Fig. 5F). Even if each cell line is plated at lower density, 1.0×10^5 cells/cm^2, the differences between the three cell lines are still observed; however, it takes more time for each TER to reach a peak (data not shown). Therefore, these data indicate that the overexpression of L-ASIP WT, but not its mutant lacking the aPKC-binding sequence, promotes TJ formation after plating without changing the rate of MDCK cell proliferation.

Induced overexpression of ASIP/PAR-3 in MDCK cells promotes insolubilization of occludin after calcium switch

Besides the development of TER, the phosphorylation and enhanced resistance to NP-40 extraction of occludin are also closely related to epithelial TJ formation in various cultured cells (Sakakibara et al., 1997). If L-ASIP WT does promote TJ formation, the biochemical behavior of occludin can be expected to be affected in MDCK cells expressing L-ASIP WT. To evaluate this possibility, we examined occludin insolubilization after Ca^{2+} switch (Gumbiner and Simons, 1986) in MDCK cells expressing L-ASIP WT or ΔPB. Culture in low (5 μM) Ca^{2+} medium disrupts cell-cell junctional complexes, and switching to normal (1.8 mM) Ca^{2+} medium triggers cadherin-mediated cell-cell contacts and a series of molecular events, including occludin insolubilization, to reconstitute junctional complexes. Confluent monolayers of MDCK cell lines were cultured in low Ca^{2+} medium for 20 hours, and then $CaCl_2$ was added back to restore the Ca^{2+} level (Ca^{2+} switch). Each cell line cultured in the presence or absence of 10 ng/ml of DC was subjected to Ca^{2+} switch. At different times after Ca^{2+} switch, total cell lysates were fractionated into NP-40-soluble and -insoluble fractions, and the amount of insoluble occludin in each cell line was evaluated by western blotting with anti-occludin antibody. The amount of protein applied to each lane for each cell line were normalized to CBB-stained tubulin levels.

As reported previously, phosphorylated and slowly migrating occludin collects preferentially in the NP-40-insoluble fraction, and there was no significant change in the total amount of occludin in any cell line examined throughout the time course (data not shown) (Sakakibara et al., 1997). In MDCK cell lines expressing L-ASIP WT, the amount of NP-40-insoluble occludin starts to increase rapidly to about 1.7-fold within 30 minutes after Ca^{2+} switch, and finally reaches about twice the level before Ca^{2+} switch (Fig. 6A, left panel; Fig. 6C, filled circles). By contrast, in cells without the induced overexpression of L-ASIP WT (DC=10 ng/ml), it takes 60 minutes to reach the same level (Fig. 6A, right panel; Fig. 6C, unfilled circles). Furthermore, the induced overexpression of L-ASIP ΔPB has no significant effect on the insolubilization of occludin after Ca^{2+} switch (Fig. 6B; Fig. 6D, filled and unfilled squares). Consistent with the above results of TER development, these data indicate that only L-ASIP WT promotes TJ formation in MDCK cells.

Taken together, these independent results evaluating TJ formation by functional and biochemical analyses clearly indicate that the overexpression of L-ASIP WT promotes TJ formation in MDCK cells. Furthermore, only L-ASIP WT, and not L-ASIP ΔPB, has such an effect, suggesting that the

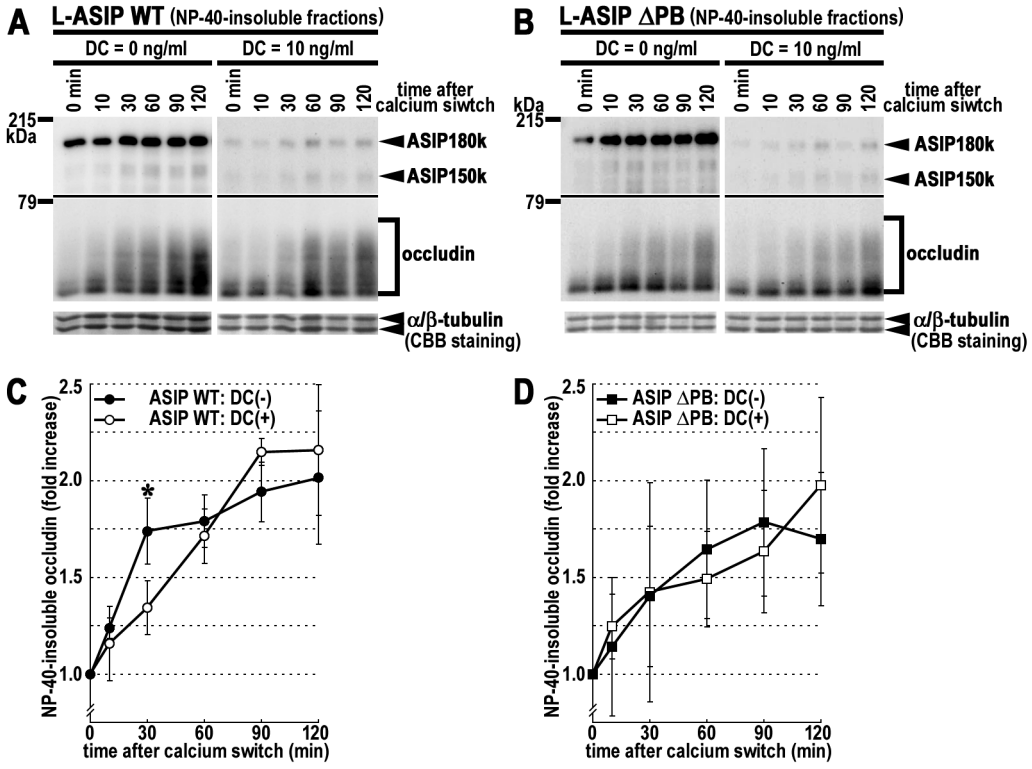

Fig. 6. Insolubilization of occludin after Ca^{2+} switch in MDCK cell lines expressing L-ASIP WT (A,C) or ΔPB (B,D). MDCK cells cultured with or without 10 ng/ml of DC were harvested at different times after Ca^{2+} switch, and the NP-40-insoluble fractions were subjected to western blot analysis with anti-ASIP (C2-3AP) or anti-occludin pAb. CBB staining of tubulins on the blotted membranes is shown as a control. The results are representative of three independent experiments. NP-40-insoluble occludin was detected by chemiluminescence ECL, and the resulting signals were quantified directly with LAS-1000 plus system (FUJI Photo Film, Tokyo, Japan) in a fluorescence image mode and normalized to the amount of tubulins in each lane (C,D). Each point is the mean±s.e.m. of three independent experiments. *P*-values were calculated with a two-sided *t*-test and statistical significance was considered at $P<0.05$ (asterisk). Induced overexpression of L-ASIP WT (C; filled circles), but not ΔPB (D; filled squares), results in the rapid accumulation of occludin in NP-40-insoluble fractions after Ca^{2+} switch.

interaction between ASIP/PAR-3 and aPKC may be involved in the promotion of TJ formation.

ASIP/PAR-3 phosphorylated at Ser827 concentrates at the most apical tip of cell-cell contacts during the restoration of cell-cell junctions

The aPKC-binding sequence in ASIP/PAR-3 includes two highly conserved serine residues (827 and 829) within the PKC phosphorylation consensus sequence (Izumi et al., 1998). Furthermore, we have recently identified Ser827 in ASIP/PAR-3 as being phosphorylated by aPKC in vivo and in vitro (Y.T.-N. and S.O., unpublished). Therefore, the above results suggesting the significance of the aPKC-binding sequence of ASIP/PAR-3 in the promotion of TJ formation imply that the phosphorylation of Ser827 is involved in this ASIP/PAR-3 function. To assess this possibility, we observed the localization of the Ser827-phosphorylated form of ASIP/PAR-3 in MDCK cells overexpressing L-ASIP WT after Ca^{2+} switch using an antibody that specifically recognizes this phosphorylated form of ASIP/PAR-3 (Fig. 7L,M). When mature cell-cell junctions are established, the immunoreactivities of Ser827-phosphorylated ASIP/PAR-3 (Fig. 7A,C, red) completely overlap overexpressed L-ASIP WT in apical cell-cell junctions (Fig. 7A-C, arrows). By contrast, 1 hour after Ca^{2+} switch, when cell-cell junctions are developing, the Ser827-phosphorylated ASIP/PAR-3 signals (Fig. 7D) are concentrated at the most apical tip of cell-cell contacts (Fig. 7F,G, filled arrowhead), while overexpressed L-ASIP WT (Fig. 7E) is still detected predominantly in a region slightly basal to the apical tip (Fig. 7F,H, unfilled arrowhead). These results imply a relationship between the localization of ASIP/PAR-3 and the phosphorylation at Ser827 during TJ formation.

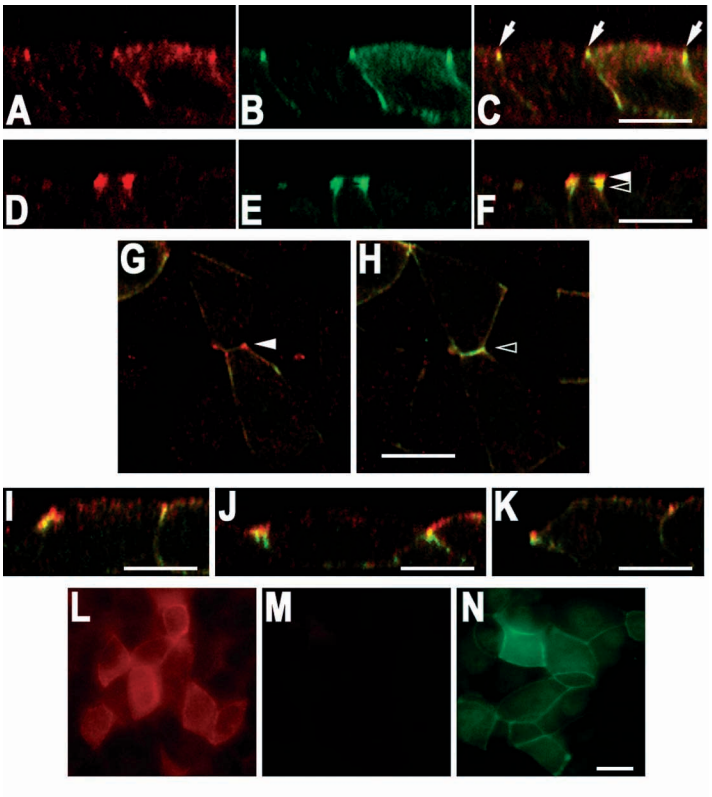

Fig. 7. Localization of Ser827 phosphorylated ASIP/PAR-3 in mature and immature cell-cell contacts. ASIP/PAR-3 phosphorylated at Ser827 (A,D) and overexpressed T7-tagged ASIP/PAR-3 (B,E) were labeled with Cy3 and FITC, respectively. Four hours after Ca^{2+} switch, the overexpressed ASIP/PAR-3 (green; B,C) in mature cell-cell contacts overlaps the immunoreactivities of ASIP/PAR-3 phosphorylated at Ser827 (red; A,C, arrows). In contrast, 1 hour after switching, the immunoreactivities for ASIP/PAR-3 phosphorylated at Ser827 predominantly occupy the most apical tip of the immature cell-cell contacts (D,F; filled arrowhead), whereas overexpressed L-ASIP WT is detected also in the region slightly basal to the apical tip (E, F; unfilled arrowhead). The merged view of an X-Z optical section is shown in F with filled and unfilled arrowheads corresponding to the levels of the X-Y optical sections shown in G and H, respectively. The distance between the two X-Y optical sections is 1.75 μm. Merged X-Z views of other representatives are shown in I, J and K. Anti-S827-P antibody strongly stains cell-cell junctions of MDCK cells expressing T7-tagged ASIP/PAR-3 (L), whereas the antigen peptide abolishes the signals (M) in cell-cell junctions where T7-tagged ASIP/PAR-3 is concentrated (N). The distribution of overexpressed T7-tagged ASIP/PAR-3 in the same field as in M is shown in N. Bars, 10 μm.

Discussion

In mammalian epithelial cells, the most apical components of the lateral junctional complex are TJs that serve as intercellular barriers to regulate paracellular permeability and function as intramembranous fences to maintain the polarization of the apical and basolateral membrane domains (Mitic and Anderson, 1998; Cereijido et al., 1998). A growing number of TJ-associated peripheral or integral proteins have been identified, and the characterized properties of these proteins provide a molecular basis for TJ formation and function. However, at present it is not fully understood how the formation of this complicated junctional structure is orchestrated in terms of the dynamic process.

We have previously identified ASIP, the mammalian homolog of *C. elegans* polarity protein PAR-3, as an epithelial TJ-associated peripheral protein (Izumi et al., 1998); however, the physiological functions of mammalian ASIP/PAR-3 remain to be clarified. In this study, we provide two lines of evidence suggesting that ASIP/PAR-3 is involved in the early phase of epithelial TJ formation. First, immunofluorescence analysis of various rat epithelial tissues shows that, in contrast to ZO-1, ASIP/PAR-3 distributes to the apical junctional complex regions of epithelial cells that do not have well-developed TJ strands (Fig. 2), and a higher level of ASIP/PAR-3 is observed in some epithelial cells with immature TJs (Fig. 2C, forestomach; Fig. 2G, small intestine). In addition, immunogold electron microscopy of epithelial cells in renal tubules reveals that ASIP/PAR-3 concentrates exclusively in the cytoplasm of the apical edge of TJ, whereas ZO-1 distributes alongside the TJ (Fig. 3). These observations indicate that, unlike ZO-1, the distribution patterns of ASIP/PAR-3 do not necessarily correlate with the level of TJ development in epithelial cells. Thus, these findings do not favor the possibility that ASIP/PAR-3 serves simply as a structural element of TJs. Second, we observed that the overexpression of L-ASIP WT in MDCK cells promotes the initial phase of TJ formation as evaluated by functional (Fig. 5; TER development measurement) as well as biochemical

(Fig. 6; occludin insolubilization) analyses. Intriguingly, the promotion of TJ formation by ASIP/PAR-3 is observed in MDCK cells overexpressing L-ASIP WT, but not those overexpressing L-ASIP ΔPB, which lacks the aPKC-binding sequence, implying that this function of ASIP/PAR-3 is mediated through the interaction with aPKC. This conclusion is further supported by our demonstration that aPKC activity is indispensable for the formation but not the maintenance of TJs in mammalian epithelial cells (Suzuki et al., 2001). Furthermore, the significance of the interaction between ASIP/PAR-3 and aPKC for TJ formation is consistent with previous reports that *C. elegans* PAR-3 and aPKC/PKC-3, or their *Drosophila* homologs, are mutually dependent on each other for their proper functions in the establishment of cell polarity (Tabuse et al., 1998; Wodarz et al., 2000). Taken together, our results strengthen the possibility that the evolutionarily conserved aPKC–ASIP/PAR-3 complex is one of the regulatory elements in mammalian epithelial TJs, and is required to promote the initial phase of TJ formation rather than serving only as a structural component.

The ultrastructural analysis of ASIP/PAR-3 localization described here is the first example of a protein that concentrates at the apical edge of TJs (Fig. 3). With respect to mammalian epithelial polarity, TJs are the borders of the apical and lateral membrane domains. In epithelial cells of arthropods, which lack TJs, the boundary between the apical and lateral membrane domains is marked by the 'marginal zone', the edge of the apical membrane domain characterized by the specific accumulation of key regulators of apical polarity such as Crumbs and Discs Lost (Tepass, 1997; Tanentzapf et al., 2000). Although it has not been shown that mammalian epithelial cells possess such a structure, the characteristic localization of ASIP/PAR-3 is reminiscent of that of Crumbs and Discs Lost. Taken together with the possible function of ASIP/PAR-3, our data suggest the intriguing hypothesis that the apical edge of TJs might be a functional analog of the marginal zone to specify membrane polarity in mammalian epithelial cells.

Accumulating experimental evidence favors the possibility of multiple steps in epithelial TJ formation. Our present data imply that the aPKC–ASIP/PAR-3 complex positively regulates epithelial TJ formation, but for which step is this complex responsible? Several lines of evidence suggest that the E-cadherin adhesion system mediates the initial organization of TJ components, including ZO-1, into primordial adherence junctions (Gumbiner et al., 1988; Rajasekaran et al., 1996; Ando-Akatsuka et al., 1999). In the next step, vinculin associated with the cadherin–αE-catenin complex serves to assemble apical actin bundles (Watabe-Uchida et al., 1998). Moreover, since there are data to indicate that ZO-1, ZO-2 and ZO-3 bind directly to occludin and claudins, which are the primary components of TJ strands, and actin filaments, it appears reasonable to speculate that ZO-1, ZO-2 and ZO-3 may be recruited from cadherin-based primordial adherens junctions to crosslink the assembled apical actin bundles and claudin-based TJ strands (Furuse et al., 1994; Haskins et al., 1998; Itoh et al., 1999; Wittchen et al., 1999). The aPKC–ASIP/PAR-3 complex, including activated aPKC, and its concentration at apical cell-cell contacts might be critical for this segregation of ZO-1 to the TJ structure from cadherin-based primordial adherens junctions. This idea is based on our previous observations and the results presented here. First, the overexpression of an aPKCλ mutant lacking kinase activity not only affects proper ASIP/PAR-3 localization, but also significantly perturbs ZO-1 localization to cell-cell junctions in MDCK cells during TJ formation without severely disturbing the localization of E-cadherin or β-catenin (Suzuki et al., 2001). Second, we demonstrate here that a relatively higher amount of ASIP/PAR-3 concentrates to cell-cell junctions in the immature epithelia of forestomach and small intestine where relatively low amounts of ZO-1 are concentrated (Fig. 2A-H). Third, we show that ASIP/PAR-3 phosphorylated at Ser827 is more concentrated at the apical tip of developing cell-cell contacts than another form of ASIP/PAR-3 without phosphorylated Ser827 (Fig. 7D-H). This Ser827 is phosphorylated by aPKC in vitro and in vivo in polarized MDCK cells (Y.T.-N. and S.O., unpublished). Lastly, our recent observations have revealed that the aPKC–ASIP/PAR-3 complex exists in the cytoplasm even in the absence of cell-cell contacts, and that it translocates to the apical cell-cell contact region very early after calcium-triggered cell-cell adhesion (Yamanaka et al., 2001). Therefore, our results, together with previously published data, allow us to speculate about the following possibility: the de novo formation of cell-cell contacts initiates the translocation of pre-existing aPKC–ASIP/PAR-3 complexes to primordial adherens junctions, and aPKC might phosphorylate ASIP/PAR-3 at Ser827 to concentrate this complex at developing apical cell-cell junctions; consequently, aPKC–ASIP/PAR-3 could promote the segregation of TJ-associating proteins, including ZO-1, from primordial adherens junctions.

Besides the peripheral proteins of TJ, occludin, claudins and junctional adhesion molecules have been identified as integral TJ membrane proteins (Furuse et al., 1993; Furuse et al., 1998a; Martin-Padura et al., 1998). Previous experimental evidence suggests that highly phosphorylated occludin co-polymerizes into claudin-based TJ strands at a relatively later phase of TJ formation, whereas non- or less-phosphorylated occludin distributes to the basolateral membrane (Sakakibara et al., 1997; Furuse et al., 1998b; Morita et al., 1998). Our present data indicate that the overexpression of ASIP/PAR-3 accelerates occludin insolubilization, which is presumably due to phosphorylation during the formation of TJ in MDCK cells (Fig. 6C). In addition, we demonstrate here the frequent localization of ASIP/PAR-3 at the basal edges of TJ as visualized by immunoelectron microscopy (Fig. 3A,B). Therefore, we propose that ASIP/PAR-3 may participate in the translocation of occludin from the basolateral membrane domain into TJ strands to establish mature TJs. Further analyses, including the targeted disruption of the aPKC and/or ASIP/PAR-3 gene, will make it possible to elucidate the hierarchy of stages in the formation of epithelial TJ and the development of epithelial polarity.

We thank Shoichiro Tsukita and Masahiko Ito (Kyoto University) for the anti-ZO-1 monoclonal antibody and helpful discussions, Michiko Ehara (Second Department of Pathology, Yokohama City University, School of Medicine) for technical help, and all the members of our laboratory (Department of Molecular Biology, Yokohama City University, School of Medicine) for stimulating discussions and helpful comments. T.H. is grateful to H. Ishikawa for her encouragement. This work was supported by grants from the Japan Society for the Promotion of Science (to S.O.) and the Ministry of Education, Science, Sports and Culture of Japan (to S.O.).

References

Ando-Akatsuka, Y., Yonemura, S., Itoh, M., Furuse, M. and Tsukita, S. (1999). Differential behavior of E-cadherin and occludin in their colocalization with ZO-1 during the establishment of epithelial cell polarity. *J. Cell. Physiol.* **179**, 115-125.

Balda, M. S. and Matter, K. (1998). Tight junctions. *J. Cell Sci.* **111**, 541-547.

Barth, A. I., Pollack, A. L., Altschuler, Y., Mostov, K. E. and Nelson, W. J. (1997). NH2-terminal deletion of beta-catenin results in stable colocalization of mutant beta-catenin with adenomatous polyposis coli protein and altered MDCK cell adhesion. *J. Cell Biol.* **136**, 693-706.

Cereijido, M., Valdes, J., Shoshani, L. and Contreras, R. G. (1998). Role of tight junctions in establishing and maintaining cell polarity. *Annu. Rev. Physiol.* **60**, 161-177.

Etemad-Moghadam, B., Guo, S. and Kemphues, K. J. (1995). Asymmetrically distributed PAR-3 protein contributes to cell polarity and spindle alignment in early *C. elegans* embryos. *Cell* **83**, 743-752.

Farquhar, M. G. and Palade, G. E. (1963) Junctional complexes in various epithelia. *J. Cell Biol.* **17**, 375-412.

Furuse, M., Hirase, T., Itoh, M., Nagafuchi, A., Yonemura, S., Tsukita, S. and Tsukita, S. (1993). Occludin: a novel integral membrane protein localizing at tight junctions. *J. Cell Biol.* **123**, 1777-1788.

Furuse, M., Itoh, M., Hirase, T., Nagafuchi, A., Yonemura, S., Tsukita, S. and Tsukita, S. (1994). Direct association of occludin with ZO-1 and its possible involvement in the localization of occludin at tight junctions. *J. Cell Biol.* **127**, 1617-1626.

Furuse, M., Fujita, K., Hiiragi, T., Fujimoto, K. and Tsukita S. (1998a). Claudin-1 and -2: novel integral membrane proteins localizing at tight junctions with no sequence similarity to occludin. *J. Cell Biol.* **141**, 1539-1550.

Furuse, M., Sasaki, H., Fujimoto, K. and Tsukita, S. (1998b). A single gene product, claudin-1 or -2, reconstitutes tight junction strands and recruits occludin in fibroblasts. *J. Cell Biol.* **143**, 391-401.

Gossen, M. and Bujard, H. (1992). Tight control of gene expression in mammalian cells by tetracycline-responsive promoters. *Proc. Natl. Acad. Sci. USA* **89**, 5547-5551.

Gumbiner, B. and Simons, K. (1986). A functional assay for proteins involved in establishing an epithelial occluding barrier: identification of a uvomorulin-like polypeptide. *J. Cell Biol.* **102**, 457-468.

Gumbiner, B., Stevenson, B. and Grimaldi, A. (1988). The role of the cell adhesion molecule uvomorulin in the formation and maintenance of the epithelial junctional complex. *J. Cell Biol.* **107**, 1575-1587.

Haskins, J., Gu, L., Wittchen, E. S., Hibbard, J. and Stevenson, B. R. (1998). ZO-3, a novel member of the MAGUK protein family found at the tight junction, interacts with ZO-1 and occludin. *J. Cell Biol.* **141**, 199-208.

Itoh, M., Furuse, M., Morita, K., Kubota, K., Saitou, M. and Tsukita, S. (1999). Direct binding of three tight junction-associated MAGUKs, ZO-1, ZO-2, and ZO-3, with the COOH termini of claudins. *J. Cell Biol.* **147**, 1351-1363.

Izumi, Y., Hirose, T., Tamai, Y., Hirai, S., Nagashima, Y., Fujimoto, T., Tabuse, Y., Kemphues, K. J. and Ohno, S. (1998). An atypical PKC directly associates and colocalizes at the epithelial tight junction with ASIP, a mammalian homologue of *Caenorhabditis elegans* polarity protein PAR-3. *J. Cell Biol.* **143**, 95-106.

Joberty, G., Petersen, C., Gao, L. and Macara, I. G. (2000). The cell-polarity protein Par6 links Par3 and atypical protein kinase C to Cdc42. *Nat. Cell Biol.* **2**, 531-539.

Jou, T. S. and Nelson, W. J. (1998). Effects of regulated expression of mutant RhoA and Rac1 small GTPases on the development of epithelial (MDCK) cell polarity. *J. Cell Biol.* **142**, 85-100.

Jou, T. S., Schneeberger, E. E. and Nelson, W. J. (1998). Structural and functional regulation of tight junctions by RhoA and Rac1 small GTPases. *J. Cell Biol.* **142**, 101-115.

Kuchinke, U., Grawe, F. and Knust, E. (1998). Control of spindle orientation in *Drosophila* by the Par-3-related PDZ-domain protein Bazooka. *Curr. Biol.* **8**, 1357-1365.

Kurihara, H., Anderson, J. M. and Farquhar, M. G. (1992). Diversity among tight junctions in rat kidney: glomerular slit diaphragms and endothelial junctions express only one isoform of the tight junction protein ZO-1. *Proc. Natl. Acad. Sci. USA* **89**, 7075-7079.

Laemmli, U. K. (1970). Cleavage of structural proteins during the assembly of the head of bacteriophage T4. *Nature* **227**, 680-685.

Lin, D., Edwards, A. S., Fawcett, J. P., Mbamalu, G., Scott, J. D. and Pawson, T. (2000). A mammalian PAR-3-PAR-6 complex implicated in Cdc42/Rac1 and aPKC signalling and cell polarity. *Nat. Cell Biol.* **2**, 540-547.

Marcial, M. A., Carlson, S. L. and Madara, J. L. (1984). Partitioning of paracellular conductance along the ileal crypt-villus axis: a hypothesis based on structural analysis with detailed consideration of tight junction structure-function relationships. *J. Membr. Biol.* **80**, 59-70.

Martin-Padura, I., Lostaglio, S., Schneemann, M., Williams, L., Romano, M., Fruscella, P., Panzeri, C., Stoppacciaro, A., Ruco, L., Villa, A. et al. (1998). Junctional adhesion molecule, a novel member of the immunoglobulin superfamily that distributes at intercellular junctions and modulates monocyte transmigration. *J. Cell Biol.* **142**, 117-127.

McLean, I. W. and Nakane, P. K. (1974). Periodate-lysine-paraformaldehyde fixative. A new fixation for immunoelectron microscopy. *J. Histochem. Cytochem.* **22**, 1077-1083.

Mitic, L. L. and Anderson, J. M. (1998). Molecular architecture of tight junctions. *Annu. Rev. Physiol.* **60**, 121-142.

Morita, K., Itoh, M., Saitou, M., Ando-Akatsuka, Y., Furuse, M., Yoneda, K., Imamura, S., Fujimoto, K. and Tsukita, S. (1998). Subcellular distribution of tight junction-associated proteins (occludin, ZO-1, ZO-2) in rodent skin. *J. Invest. Dermatol.* **110**, 862-826.

Rajasekaran, A. K., Hojo, M., Huima, T. and Rodriguez-Boulan, E. (1996). Catenins and zonula occludens-1 form a complex during early stages in the assembly of tight junctions. *J. Cell Biol.* **132**, 451-463.

Sakakibara, A., Furuse, M., Saitou, M., Ando-Akatsuka, Y. and Tsukita, S. (1997). Possible involvement of phosphorylation of occludin in tight junction formation. *J. Cell Biol.* **137**, 1393-1401.

Saxon, M. L., Zhao, X. and Black, J. D. (1994). Activation of protein kinase C isozymes is associated with post-mitotic events in intestinal epithelial cells in situ. *J. Cell Biol.* **126**, 747-763.

Schnabel, E., Anderson, J. M. and Farquhar, M. G. (1990). The tight junction protein ZO-1 is concentrated along slit diaphragms of the glomerular epithelium. *J. Cell Biol.* **111**, 1255-1263.

Staehelin, L. A. (1973). Further observations on the fine structure of freeze-cleaved tight junctions. *J. Cell Sci.* **13**, 763-786.

Stevenson, B. R., Siliciano, J. D., Mooseker, M. S. and Goodenough, D. A. (1986). Identification of ZO-1: a high molecular weight polypeptide associated with the tight junction (zonula occludens) in a variety of epithelia. *J. Cell Biol.* **103**, 755-766.

Suzuki, A., Yamanaka, T., Hirose, T., Manabe, M., Mizuno, K., Akimoto, K., Izumi, Y., Ohnishi, T. and Ohno, S. (2001). Atypical PKC is involved in the evolutionarily conserved PAR protein complex and plays a critical role to establish epithelia-specific junctional structures. *J. Cell Biol.* **152**, 1183-1196.

Tabuse, Y., Izumi, Y., Piano, F., Kemphues, K. J., Miwa, J. and Ohno, S. (1998). Atypical protein kinase C cooperates with PAR-3 to establish embryonic polarity in *Caenorhabditis elegans*. *Development* **125**, 3607-3614.

Tanentzapf, G., Smith, C., McGlade, J. and Tepass, U. (2000). Apical, lateral, and basal polarization cues contribute to the development of the follicular epithelium during *Drosophila* oogenesis. *J. Cell Biol.* **151**, 891-904.

Tepass, U. (1997). Epithelial differentiation in *Drosophila*. *Bioessays* **19**, 673-682.

Tsukita, S., Furuse, M. and Itoh, M. (1999). Structural and signalling molecules come together at tight junctions. *Curr. Opin. Cell Biol.* **11**, 628-633.

Watabe-Uchida, M., Uchida, N., Imamura, Y., Nagafuchi, A., Fujimoto, K., Uemura, T., Vermeulen, S., van Roy, F., Adamson, E. D. and Takeichi, M. (1998). α-Catenin-vinculin interaction functions to organize the apical junctional complex in epithelial cells. *J. Cell Biol.* **142**, 847-857.

Wittchen, E. S., Haskins, J. and Stevenson, B. R. (1999). Protein interactions at the tight junction. Actin has multiple binding partners, and ZO-1 forms independent complexes with ZO-2 and ZO-3. *J. Biol. Chem.* **274**, 35179-35185.

Wodarz, A., Ramrath, A., Grimm, A. and Knust, E. (2000). *Drosophila* atypical protein kinase C associates with Bazooka and controls polarity of epithelia and neuroblasts. *J. Cell Biol.* **150**, 1361-1374.

Yamanaka, T., Horikoshi, Y., Suzuki, A., Sugiyama, Y., Kitamura, K., Maniwa, R., Nagai, Y., Yamashita, A., Hirose, T., Ishikawa, H. and Ohno, S. (2001). PAR-6 regulates aPKC activity in a novel way and mediates cell-cell contact-induced formation of the epithelial junctional complex. *Genes Cells* **6**, 721-731.

Yeaman, C., Grindstaff, K. K. and Nelson, W. J. (1999). New perspectives on mechanisms involved in generating epithelial cell polarity. *Physiol. Rev.* **79**, 73-98.